inter.noise
HAMBURG 2016

A scaling method for vibrating structures using global sensitivity analysis

Christian ADAMS[1], Joachim BÖS[2], and Tobias MELZ[3]
System Reliability, Adaptive Systems, and Machine Acoustics SAM,
Technische Universität Darmstadt, Germany

ABSTRACT

Scaling vibrating structures is a common engineering problem, e.g., large structures that are investigated on a laboratory scale model. Those investigations require scaling laws to scale up the laboratory model to the original structure or vice versa. Scaling laws are usually derived from a similitude analysis of the equations of motion. Both methods are hardly applied to more complex structures, because the influence of design parameters on the structural vibrations is unknown. This paper proposes a method to derive scaling laws for vibrating structures based on a global sensitivity analysis (GSA). GSA covers the design parameter space as a whole and can predict structural vibrations depending on the effects of design parameters and the effects of interactions between design parameters. After performing GSA the scaling law is set up, and vibrations can be calculated. The method will be exemplified for a vibrating simply supported rectangular plate. The accuracy of the scaling law is analyzed by comparing it to a scaling law derived from the equations of motion. Using the effects of design parameters as well as their interactions will increase the accuracy of the scaling law. The method can be applied to more complex structures in a next step.

Keywords: vibration, similitude, global sensitivity analysis
I-INCE Classification of Subjects Number: 42

1. INTRODUCTION

Vibroacoustic investigations of structures are very extensive in some cases, e.g., because of the structure's size. Therefore, a laboratory model will be used instead, and the results from the laboratory model will be scaled up to the original structure or vice versa. This scaling procedure requires an appropriate scaling law that is usually derived from a similitude analysis of the equations of motion [1]. This approach is used by several authors to derive scaling laws of simple vibrating structures. Soedel [2] approximates the scaling laws for vibrating shells using the governing equations of shell theory and applies them to a cylindrical shell. Rezaeepazhand [3] applies scaling laws to a cylindrical shell made from composite material. He concludes that the scaling law is suitable to design small-scale models from a larger original structure. Wu [4] proposes *complete-similitude scale models* to analyse the vibration response of a flat rectangular plate excited by both a dynamic point load and a moving point load. The natural frequencies as well as the time-domain vibration response of the original structure can be predicted accurately by using the scaled model and the scaling law. In a further study [5] Wu extends the method to rectangular plates excited by several *circular-moving* point loads. De Rosa [6] develops the *asymptotic scaled modal analysis*, i.e., a hybrid approach that combines a similitude analysis with both modal analysis and statistical energy analysis. Several structures are investigated, e.g., rectangular plates or assemblies of plates [7]. Furthermore, De

[1]adams@sam.tu-darmstadt.de
[2]boes@sam.tu-darmstadt.de
[3]melz@sam.tu-darmstadt.de

Rosa investigates exactly and distorted scaled plates [8]. Exactly scaled plates are scaled equally in all dimensions. In this case the vibrations are predicted exactly by the scaling law. Distorted scaled plates have different scaling factors for each dimension. Therefore, the scaling law approximates the vibrations. De Rosa concludes that the approximation is sufficient for engineering purposes [8].

Thus, scaling laws are suitable for predicting the vibrations of an original structure from those of a scaled model if the equation of motion is known. However, those equations of motion do not exist for practical vibroacoustic engineering problems, e.g., for gear boxes or electrical machines. Obtaining a similitude-based scaling law might be possible, but its derivation is extensive. Therefore, this paper proposes an approach for obtaining scaling laws that is based on a global sensitivity analysis (GSA). In order to validate the feasibility of such a sensitivity-based scaling law, this paper derives scaling laws for a vibrating rectangular plate by both similitude analysis and GSA.

2. MODEL SET UP

The sound power $P(f)$ of machinery excited by a dynamic force can be calculated from the fundamental equation of machine acoustics [9]

$$P(f) = \tilde{F}^2(f) S h_T^2 \sigma \rho_\mathrm{a} c_\mathrm{a}, \tag{1}$$

with $\tilde{F}^2(f)$, Sh_T^2, σ being the dynamic excitation force, the mean squared transfer admittance, and the radiation efficiency, respectively. $\rho_\mathrm{a} c$ is the acoustic impedance described by the air density ρ_a and the speed of sound in air c_a.

In this paper a simply supported rectangular plate is investigated. Fig. 1 shows the plate with its dimensions a,b, and h as well as the excitation that is assumed to be a single point load acting at the position (x_0, y_0). The force excites the plate harmonically at its natural frequencies. In the first step, only the structural vibrations are investigated. A scaling law for the sound radiation is a further step that is not within the scope of this paper. The natural frequencies $f_{m,n}$ and the mean squared transfer admittance Sh_T^2 describe the structural vibrations and are chosen as responses of the scaling laws. The natural frequencies $f_{m,n}$ of the simply supported rectangular plate are

$$f_{m,n} = \frac{\omega_{m,n}}{2\pi} = \frac{\pi}{2} h \sqrt{\frac{E}{12\rho\left(1-\mu^2\right)}} \left(\left(\frac{m}{a}\right)^2 + \left(\frac{n}{b}\right)^2 \right), \tag{2}$$

with E, ρ, and μ being the Young's modulus, the mass density, and the Poisson ratio, respectively. m and n are integer values denoting the m,n-th mode shape of the rectangular plate [10].

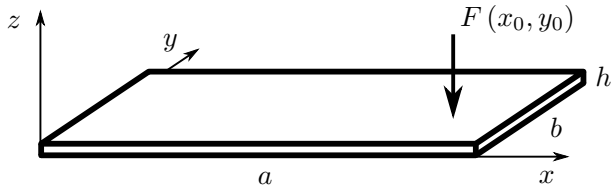

Figure 1 – simply supported rectangular plate excited by a single point load

The mean squared transfer admittance is

$$Sh_T^2 = S \frac{\overline{\tilde{v}^2}}{\tilde{F}^2}, \tag{3}$$

with the mean squared vibration velocity $\overline{\tilde{v}^2}$, the force $\tilde{F}^2$, and the surface $S = ab$ [11]. The mean squared velocity is

$$\overline{\tilde{v}^2} = \frac{1}{S} \int_S \left|\underline{\tilde{v}}(x,y)\right|^2 \mathrm{d}S, \tag{4}$$

with the complex velocities $\underline{\tilde{v}}(x,y)$. The complex velocities of the vibrating plate can be expressed as

$$\underline{\tilde{v}}(x,y) = \frac{4\tilde{F}i\omega}{\rho abh}\sum_{m=1}^{\infty}\sum_{n=1}^{\infty}\frac{\sin\left(\frac{m\pi x_0}{a}\right)\sin\left(\frac{n\pi y_0}{b}\right)}{\omega_{m,n}^2-\omega^2+i\eta\omega_{m,n}^2}\sin\left(\frac{m\pi x}{a}\right)\sin\left(\frac{n\pi y}{b}\right), \tag{5}$$

with the excitation force $\tilde{F}$, the excitation frequency $\omega = 2\pi f$, and the loss factor η [10]. Inserting the position (x_0, y_0) for x and y into Eqs. (4) and (5), the mean squared transfer admittance becomes [12]

$$Sh_T^2 = \frac{f^2}{\pi^2\rho^2h^2ab}\sum_{m=1}^{\infty}\sum_{n=1}^{\infty}\frac{\sin^2\left(\frac{m\pi x_0}{a}\right)\sin^2\left(\frac{n\pi y_0}{b}\right)}{\left(f_{m,n}^2-f^2\right)^2+\eta^2f_{m,n}^4}. \tag{6}$$

In the next sections, the scaling laws for $f_{m,n}$ and Sh_T^2 are derived from both similitude analysis and GSA.

2.1 Similitude-based scaling laws

The general procedure for obtaining a scaling law from an equation of motion can be found in literature, e.g., [1]. Fig. 2 shows the approach used in this paper that is based on [1]. First, a list of

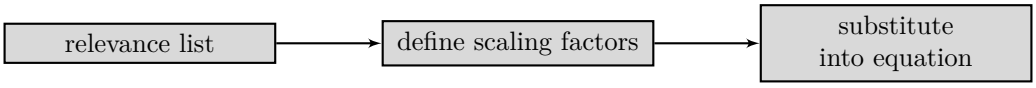

Figure 2 – schematic work flow for obtaining a similitude-based scaling law

relevant parameters is obtained by rewriting the equations of the responses in a general functional format

$$f_{m,n} = \mathfrak{f}\left(a,b,h,E,\rho,\mu\right) \tag{7}$$

for the natural frequencies from Eq. (2) and

$$Sh_T^2 = \mathfrak{f}\left(a,b,h,x_0,y_0,\rho,\eta,f\right) \tag{8}$$

for the mean squared transfer admittance from Eq. (6). $\mathfrak{f}(\ldots)$ denotes that the responses are a function of the parameters listed in parentheses. According to Fig. 2 the next step is to define the scaling factors for each parameter in Eqs. (7) and (8). Therefore, the scaling factor ϕ_ξ is defined as

$$\phi_\xi = \frac{\xi'}{\xi} \quad\Leftrightarrow\quad \xi' = \phi_\xi\xi, \tag{9}$$

with ξ being the parameters listed in Eqs. (7) and (8) that belong to the original rectangular plate and ξ' being the corresponding parameters of a scaled model.[1] Inserting the scaling factors into Eq. (2) yields

$$f'_{m,n} = \phi_h\sqrt{\frac{\phi_E}{\phi_\rho}}\frac{\pi}{2}h\sqrt{\frac{E}{12\rho\left(1-\phi_\mu\mu^2\right)}}\left(\left(\frac{m}{\phi_a a}\right)^2+\left(\frac{n}{\phi_b b}\right)^2\right). \tag{10}$$

In analogy, the mean squared transfer admittance $Sh_T'^2$ from Eq. (6) becomes

$$Sh_T'^2 = \frac{1}{\phi_\rho^2\phi_h^2\phi_a\phi_b}\frac{f^2}{\pi^2\rho^2h^2ab}\sum_{m=1}^{\infty}\sum_{n=1}^{\infty}\frac{\sin^2\left(m\pi p\right)\sin^2\left(n\pi q\right)}{\left(\phi_f^2f_{m,n}^2-f^2\right)^2+\phi_\eta\eta^2\phi_f^4f_{m,n}^4}, \tag{11}$$

with $p = x/a$ and $q = y/b$ being dimensionless coordinates. Eqs. (10) and (11) are the scaling laws for the natural frequencies and for the mean squared transfer admittance of the rectangular

[1]Note, $\phi_\xi > 1$ means that the original plate is scaled up, and $\phi_\xi < 1$ means that the original plate is scaled down.

plate. Assuming that the material of the original plate and its scaled model remains the same, i.e., $\phi_E = \phi_\rho = \phi_\mu = \phi_\eta = 1$, and that the plate is scaled equally in length and width, i.e., $\phi_a = \phi_b = \phi_l$, leads to

$$f'_{m,n} = \frac{\phi_h}{\phi_l^2}\frac{\pi}{2}h\sqrt{\frac{E}{12\rho\left(1-\mu^2\right)}}\left(\left(\frac{m}{a}\right)^2+\left(\frac{n}{b}\right)^2\right) = \frac{\phi_h}{\phi_l^2}f_{m,n}. \tag{12}$$

From Eq. (12) the scaling factor $\phi_f = \phi_h/\phi_l^2$ can be derived, and inserting it into Eq. (11) leads to

$$Sh'^2_T = \left(\frac{\phi_l}{\phi_h}\right)^6 \frac{f^2}{\pi^2\rho^2h^2ab}\sum_{m=1}^{\infty}\sum_{n=1}^{\infty}\frac{\sin^2\left(m\pi p\right)\sin^2\left(n\pi q\right)}{\left(f_{m,n}^2-\left(\frac{\phi_l^2 f}{\phi_h}\right)^2\right)^2+\eta^2 f_{m,n}^4}. \tag{13}$$

These scaling laws match those from literature, e.g., [8] and [12]. Thus, they are feasible to validate the sensitivity-based scaling laws that are derived in the following section.

2.2 Sensitivity-based scaling laws

GSA investigates how a change of design parameters of a model affects the desired model outputs (i.e., the responses). Therefore, the design parameters are altered in a defined manner and their effect on the responses is obtained [13]. The effect of a design parameter is defined as the averaged change of the response that is caused by altering the design parameter value [14]. Applying the work flow shown in Fig. 3 leads to the scaling laws of the rectangular plate.

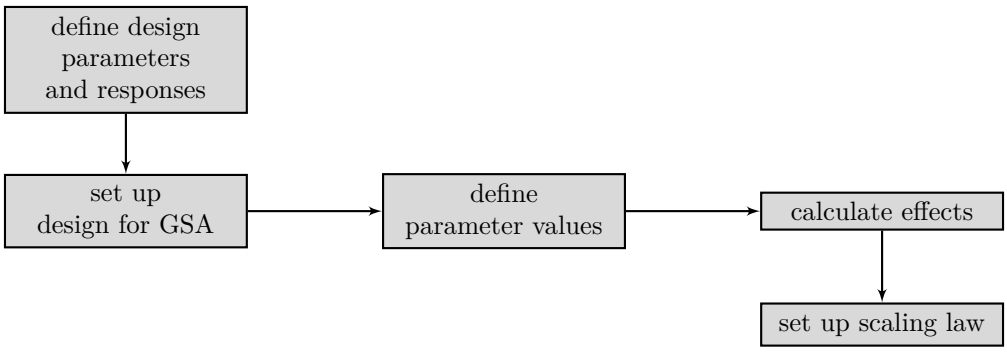

Figure 3 – schematic work flow for obtaining a sensitivity-based scaling law

The first step defines the design parameters and the responses. In coincidence to the similitude-based scaling laws in Eqs. (12) and (13), the design parameters are the length a, the width b, and the thickness h. The responses are the fundamental frequency $f_{1,1}$ and the mean squared transfer admittance at the fundamental frequency $Sh'^2_T\left(f_{1,1}\right)$. However, in GSA responses that are single values are preferred to those depending on another parameter (e.g., a frequency response). The next step defines the methodology how the design parameters are altered. Here, a 2^k full factorial design including an additional central point is applied, with k being the number of design parameters. The full factorial design contains all possible combinations of design parameters and a central point that is located in the middle of the design space. Each design parameter has two levels: the lower level $(-)$ and the upper level $(+)$. The central point has the level 0. Therefore, a full factorial design with 3 design parameters leads to a cubic design space as shown in Fig. 4(a) with a total number of $m = 2^3 + 1 = 9$ points. Next, the lower and upper levels of the full factorial design are assigned to specific values of the design parameters. Besides the design parameters itself, an interaction between design parameters can affect the responses as well, i.e., the effect of a design parameter depends on the level of another design parameter (interacting parameters) [14]. Interacting parameters are obtained by generating all possible products of the design parameters. Fig. 4(b) shows the factorial

design used for the rectangular plate including the levels of both design parameters and interacting parameters. The effect E_k of the k-th design parameter or interaction can be calculated from

$$E_k = \frac{2}{m} \sum_{j=1}^{m} \operatorname{sgn}(j,k)\, Y_j, \tag{14}$$

with $\operatorname{sgn}(j,k)$ denoting the sign in the j-th row and the k-th column of the full factorial design in Fig. 4(b). Y_j is the response of the j-th row [14]. The scaling law is obtained using the effects

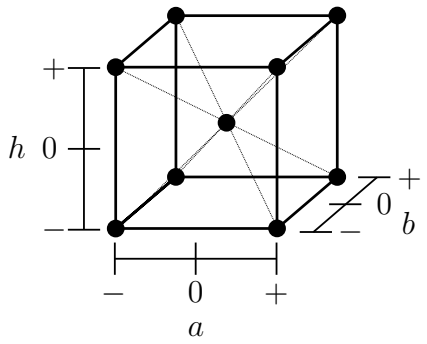

(a)

no.	**design parameter**			**interacting parameters**			
j	a	b	h	ab	ah	bh	abh
1	(−)	(−)	(−)	(+)	(+)	(+)	(−)
2	(+)	(−)	(−)	(−)	(−)	(+)	(+)
3	(−)	(+)	(−)	(−)	(+)	(−)	(+)
4	(+)	(+)	(−)	(+)	(−)	(−)	(−)
5	(−)	(−)	(+)	(+)	(−)	(−)	(+)
6	(+)	(−)	(+)	(−)	(+)	(−)	(−)
7	(−)	(+)	(+)	(−)	(−)	(+)	(−)
8	(+)	(+)	(+)	(+)	(+)	(+)	(+)
9	(0)	(0)	(0)	(0)	(0)	(0)	(0)

(b)

Figure 4 – 2^3 full factorial design for the rectangular plate

calculated from Eq. (14) and a model approach. In Eqs. (2) and (6) the design parameters have a quadratic influence on the responses. Therefore, a quadratic model approach is chosen. Let $X = \{a, b, h, ab, bh, abh\}$ be the set of inputs for the model. The quadratic model becomes

$$Y = \beta_0 + \sum_{k=1}^{n} \beta_k X_k + \sum_{k=1}^{n} \gamma_k X_k^2 + \varepsilon. \tag{15}$$

β_0 is the intercept, β_k and γ_k denote the coefficients of the k-th input from the set X, Y is the desired response, and ε is the error. The coefficients β_k and γ_k can be estimated by the least squares method. The quality of the fitted scaling law is estimated by the coefficient of determination R^2. It is defined as

$$R^2 = 1 - \frac{SS_{\text{res}}}{SS_{\text{tot}}}, \tag{16}$$

with the total sum of squares SS_{tot} and the residual sum of squares SS_{res}. Thus, R^2 describes the share of the variance that can be explained by the model. If $R^2 = 1$ the model exactly fits the data points, but predictions between the data points are not necessarily exact [14].

3. RESULTS

The original rectangular plate has the design parameters, the excitation force, and the material properties listed in Table 1. It is known from literature, e.g. [8], that the similitude-based scaling laws in Eqs. (12) and (13) exactly predict the responses. Therefore, the similitude-based scaling law is the reference solution that is used to validate the sensitivity-based scaling law. The values of the design parameters are varied from −20% to +20%. This corresponds to the scaling factors of the similitude-based scaling law of 0.8 and 1.2 (see Table 2). Note, that the position of the excitation force remains the same relative to the length and width of the rectangular plate. This will ensure that all scaled models are comparable to the original plate.

Table 1 – design parameters, excitation force, and material properties of the rectangular plate

parameter	**nomenclature**	**value**	**unit**
length	a	870	mm
width	b	620	mm
thickness	h	5	mm
excitation position	x_0	$0.885a$	–
excitation position	y_0	$0.161b$	–
excitation magnitude	$\|F\|$	1	N
Young's modulus	E	$2.04 \cdot 10^{11}$	$\mathrm{N/m^2}$
Poisson's ratio	μ	0.3	–
mass density	ρ	7850	$\mathrm{kg/m^3}$
loss factor	η	0.005	–

Table 2 – scaling factors and the corresponding design parameter values of the scaled plates

design parameter	**scaling factor**	**value**	**scaling factor**	**value**
a	$\phi_l = 0.8$	696 mm	$\phi_l = 1.2$	1044 mm
b	$\phi_l = 0.8$	496 mm	$\phi_l = 1.2$	744 mm
h	$\phi_h = 0.8$	4 mm	$\phi_h = 1.2$	6 mm

The effects of the design parameters on the responses are analyzed first to validate the results from the GSA. The effects of the design parameters on $f_{1,1}$ are shown in Fig. 5(a). They can be explained using Eq. (2):

- The effects E_a and E_b are negative, because they are in the denominator in Eq. (2).
- The effect $E_b \approx 2E_a$; the aspect ratio is $a/b \approx 1.4$ and $f_{1,1} \propto 1/b^2$. Therefore, the effect of b is $1.4^2 \approx 2$ times higher than the effect of a.
- $f_{1,1}$ increases linearly with h, thus, h has a positive effect on $f_{1,1}$.
- The interactions ah and bh are found if Eq. (2) is expanded, thus, they have an effect on $f_{1,1}$. The interactions ab and abh are not in Eq. (2). As a consequence they do not affect $f_{1,1}$.

The effects on the mean squared transfer admittance $Sh_T^2(f_{1,1})$ are shown in Fig. 5(b). They are explained by taking Eq. (6) into account:

- The plate thickness h has the highest effect, because $Sh_T^2 \propto h^{-2}$.
- Again, due to $a/b \approx 1.4$, b has a higher effect on Sh_T^2 than a.
- The interacting effects ab, ah, bh, and abh are found in the denominator of Eq. (6) and, thus, affect Sh_T^2 as well.

The sum of negative effects in Fig. 5 has a higher magnitude than the sum of positive effects for both responses. Therefore, the responses decrease if all design parameters increase equally. This can be confirmed quantitatively by comparing the similitude-based scaling law and the sensitivity-based scaling law. If all design parameters are scaled equally, i.e., $\phi_l = \phi_h = \phi$, Eq. (12) becomes

$$f'_{1,1} = \phi^{-1} f_{1,1}. \tag{17}$$

Fig. 6(a) shows the fundamental frequency $f_{1,1}$ against the scaling factor ϕ obtained from the similitude analysis (Eq. (17)) and the predicted responses from the sensitivity-based scaling law that

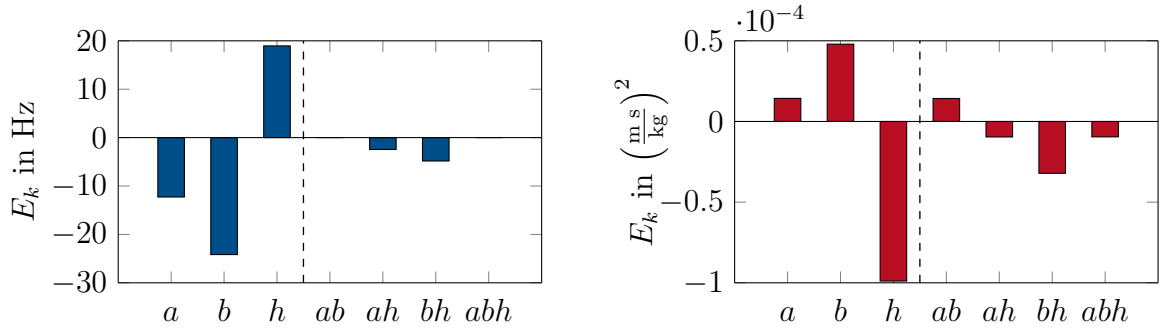

(a) effects on $f_{1,1}$ (b) effects on $Sh_T^2(f_{1,1})$

Figure 5 – effect of the design parameters and effects of the interactions between the design parameters on the responses

is fitted with $R^2 = 1$. The sensitivity-based scaling law matches the reference from the similitude-based scaling law. Therefore, the quadratic model is sufficient to predict $f_{1,1}$. Fig. 6(b) shows the results of the mean squared transfer admittance $Sh_T^2(f_{1,1})$. In this case, Eq. (13) becomes

$$Sh_T'^2 = \frac{f^2}{\pi^2 \rho^2 h^2 ab} \sum_{m=1}^{\infty} \sum_{n=1}^{\infty} \frac{\sin^2(m\pi p)\sin^2(n\pi q)}{\left(f_{m,n}^2 - \phi^2 f^2\right)^2 + \eta^2 f_{m,n}^4}. \tag{18}$$

The sensitivity-based scaling law is fitted with $R^2 = 1$ as well. Therefore, the sensitivity-based scaling law exactly predicts $Sh_T^2(f_{1,1})$ at the points of the full factorial design, i.e., for the scaling factors of 0.8, 1 and 1.2. At other points of the design space the sensitivity-based scaling law approximates the similitude-based scaling law with sufficient accuracy. In this case, the prediction is not exact because the order of the sensitivity-based scaling law is 2, whereas the similitude-based scaling law in Eq. (18) is of order 4. In a next step, the scaling factor ϕ_l is set to 1 and only ϕ_h is

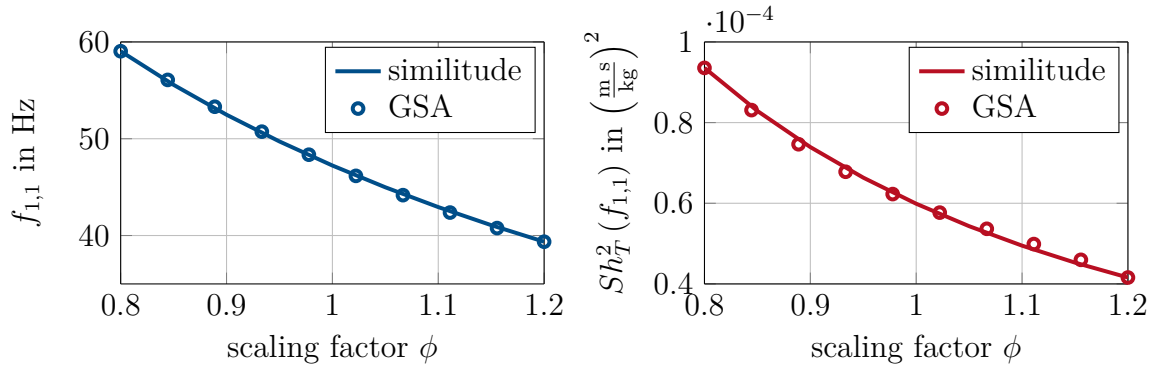

(a) (b)

Figure 6 – similitude-based scaling law and sensitivity-based scaling law for the design parameters being equally scaled

altered. In this case the similitude-based scaling law for $f_{1,1}$ (see Eq. (12)) is

$$f_{1,1}' = \phi_h f_{1,1}, \tag{19}$$

i.e., $f_{1,1}$ increases linearly with h as shown in Fig. 7(a). In the vicinity of $\phi_h = 1$ the sensitivity-based scaling law predicts the similitude-based scaling law with sufficient accuracy. The error of the approximation increases at the edges of the design space and reaches approx. 2% and 3% for

$\phi_h = 1.2$ and $\phi_h = 0.8$, respectively. For $Sh_T^2\left(f_{1,1}\right)$ Eq. (12) becomes

$$Sh_T'^2 = \phi_h^{-6} \frac{f^2}{\pi^2 \rho^2 h^2 ab} \sum_{m=1}^{\infty} \sum_{n=1}^{\infty} \frac{\sin^2\left(m\pi p\right) \sin^2\left(n\pi q\right)}{\left(f_{m,n}^2 - \left(\frac{f}{\phi_h}\right)^2\right)^2 + \eta^2 f_{m,n}^4}. \tag{20}$$

Thus, an increasing scaling factor ϕ_h causes the mean squared transfer admittance to decrease as shown in Fig. 7(b). Again, the sensitivity-based scaling law approximates well in the vicinity of $\phi_h = 1$. At $\phi_h = 0.8$ and $\phi_h = 1.2$ the error becomes 21% and 85%, respectively. Therefore, the quadratic model of the sensitivity-based scaling law is not sufficient to predict the mean squared transfer admittance.

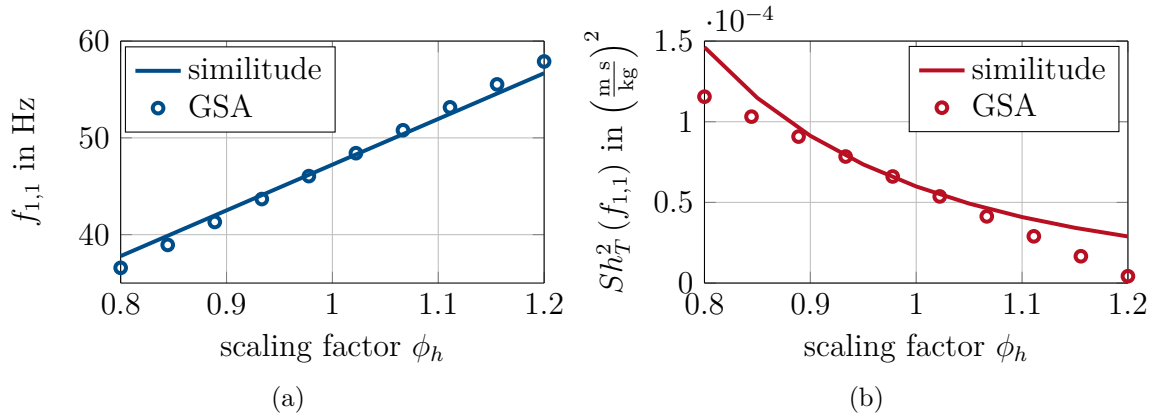

Figure 7 – similitude-based scaling law and sensitivity-based scaling law for the thickness being scaled, $\phi_l = 1$

4. SUMMARY AND CONCLUSIONS

In this paper, scaling laws are derived for a vibrating rectangular plate with simply supported edges. The scaling laws are obtained from a similitude analysis and from a global sensitivity analysis (GSA). The scaling laws are used to predict two responses: the fundamental frequency of the plate and its corresponding mean squared transfer admittance depending on the design parameters length, width, and thickness of the plate. It is known that the similitude-based scaling laws exactly predict the responses [8]. Thus, they are used to validate the sensitivity-based scaling laws. The sensitivity-based scaling laws are obtained from the results of a full factorial design. By analyzing the effects of the design parameters on the responses, the results can be validated qualitatively. Then, the sensitivity-based scaling laws are obtained by fitting quadratic models to the responses. The sensitivity-based scaling laws are found to approximate the similitude-based scaling laws sufficiently if all design parameters are scaled equally. If only the thickness of the plate is scaled, the fundamental frequency can be approximated with an error of 3%, which is still sufficient for engineering purposes. Approximating the mean squared transfer admittance with sufficient accuracy will require another model approach, e.g., of higher order.

It can be concluded from the investigations in this paper that the sensitivity-based scaling laws can be used to predict the vibration response of the rectangular plate. However, both similitude analysis and sensitivity analysis have their benefits and drawbacks that will be briefly discussed in the following based on the results of this paper. In similitude analysis the focus is on how to derive the scaling law based on the physical relations of the investigated system. The main challenge is that similitude analysis lacks a standard procedure or "algorithm" that leads to the scaling law. This is

crucial if the investigated systems are getting more and more complex, because the effort to derive the scaling laws increases. But similitude-based scaling laws might reduce the effort to investigate those complex structures, e.g., a large structure can be investigated in a laboratory scale and the scaling law is used to scale up the results to the original structure. Thus, similitude-based scaling laws are efficient tools in engineering if they are known. On the other hand, the sensitivity analysis is useful to obtain the effects of design parameters on the response of systems, although they might be complex. Using a model approach (e.g., linear, quadratic) it is always possible to fit the responses. However, this fitted model is not necessarily representing the physical relation between the design parameters and the responses. If the procedure is implemented it can be algorithmized. Thus, the effort to derive the scaling laws is reduced. But the sensitivity analysis requires an increased calculation effort and, therefore, might be inefficient. The benefits and drawbacks of both similitude analysis and sensitivity analysis are summarized in Table 3. It can be concluded that the benefits and drawbacks complement each other. Therefore, future research focuses on how to use the benefits of both similitude analysis and sensitivity analysis to derive scaling laws for vibrating structures.

Table 3 – summary of benefits and drawbacks of similitude analysis and sensitivity analysis

similitude-based scaling laws	**sensitivity-based scaling laws**
+ based on physical relations	+ reduced effort for deriving scaling laws
+ efficient for scaling problems	+ procedure can be implemented as algorithm
− increased effort for deriving scaling laws	− not based on physical relations
− lacks a standard procedure	− increased calculation effort

ACKNOWLEDGEMENTS

The authors would like to gratefully acknowledge Steffen Ochs and Philipp Neubauer for the valuable discussion and for the critical review of this manuscript.

REFERENCES

[1] W.E. Baker, P.S. Westine, and F.T. Dodge. *Similarity methods in engineering dynamics: theory and practice of scale modeling.* Elsevier, Amsterdam, 2 edition, 1991.

[2] W. Soedel. Similitude approximations for vibrating thin shells. *The Journal of the Acoustical Society of America*, 49(5):1535–1541, 1971.

[3] J. Rezaeepazhand and G.J. Simitses. Design of Scaled Down Models for Predicting Shell Vibration Repsonse. *Journal of Sound and Vibration*, 195:301–311, 1996.

[4] J. Wu. The complete-similitude scale models for predicting the vibration characteristics of the elastically restrained flat plates subjected to dynamic loads. *Journal of Sound and Vibration*, 268(5):1041–1053, 2003.

[5] J. Wu. Prediction of the dynamic characteristics of an elastically supported full-size flat plate from those of its complete-similitude scale model. *Computers & Structures*, 84(3-4):102–114, 2006.

[6] S. De Rosa and F. Franco. A scaling procedure for the response of an isolated system with high modal overlap factor. *Mechanical Systems and Signal Processing*, 22(7):1549–1565, 2008.

[7] S. De Rosa, F. Franco, and T. Polito. Structural similitudes for the dynamic response of plates and assemblies of plates. *Mechanical Systems and Signal Processing*, 25(3):969–980, 2011.

[8] S. De Rosa, F. Franco, and V. Meruane. Similitudes for the structural response of flexural plates. *Proceedings of the Institution of Mechanical Engineers, Part C: Journal of Mechanical Engineering Science*, 230(2):174 – 188, 2015.

[9] H. Hanselka and J. Bös. Maschinenakustik (machine acoustics). In K.H. Grote and J. Feldhusen, editors, *Dubbel – Taschenbuch für den Maschinenbau (Handbook of Mechanical Engineering)*, chapter O3, pages O30 – O41. Springer, Berlin, 2014.

[10] A.W. Leissa. *Vibration of plates*. NASA SP-160. Scientific and Technical Information Division, National Aeronautics and Space Administration, 1969.

[11] L. Cremer and M. Heckl. *Structure-borne sound: structural vibrations and sound radiation at audio frequencies*. Springer, Berlin, 3rd edition, 2013.

[12] F. G. Kollmann, F. Schösser, and R. Angert. *Praktische Maschinenakustik (practical machine acoustics)*. Springer, Berlin, 2006.

[13] A. Saltelli, M. Ratto, T. Andres, F. Campolongo, J. Cariboni, D. Gatelli, M. Saisana, and S. Tarantola. *Global Sensitivity Analysis: The Primer*. John Wiley & Sons, Chichester, 2008.

[14] D.C. Montgomery. *Design and Analysis of Experiments*. John Wiley & Sons, Hoboken, 2009.